Available online at www.sciencedirect.com
SCIENCE DIRECT
Polymer 46 (2005) 9296–9303
polymer
www.elsevier.com/locate/polymer

Polyimide foams from powder: Experimental analysis of competitive diffusion phenomena

Camilo I. Cano[a,*], Erik S. Weiser[b], Thein Kyu[a], R. Byron Pipes[c]

[a]Department of Polymer Engineering, The University of Akron, Akron, OH 44325-0301, USA
[b]NASA Langley Research Center, Hampton, VA 23681, USA
[c]School of Materials Engineering, Aeronautics and Astronautics, and Chemical Engineering, Purdue University, West Lafayette, IN 47907-2044, USA

Received 21 February 2005; received in revised form 13 July 2005; accepted 18 July 2005
Available online 8 August 2005

Abstract

In the present study, various diffusive processes have been investigated during foaming of powdered precursors of polyimide. A detailed analysis of the powdered precursor's characteristics allows for an enhanced morphological understanding of the resulting microstructures and foam unit cell. Parameters that are central to the foaming process such as particle morphology, volatile concentration and sorption–desorption processes are evaluated. Isothermal and non-isothermal desorption experiments have been carried out by thermogravimetric analysis (TGA), and specific diffusive processes have been correlated to thermodynamic and kinetic transitions by means of modulated differential scanning calorimetry (MDSC) of the corresponding materials. It was found that two primary fluxes of volatiles, one out of the external surface of the particles (responsible for volatile desorption) and the other into the growing bubble (responsible for vapor supersaturation inside the bubble) compete against each other creating a competitive scenario that becomes the controlling factor for potential inflation within the precursor particles.

Keywords: Polyimide; Foam; Powder

1. Introduction

Polymers with imide groups in their backbone possess very special properties that make them prime candidates when high temperature material performance is required. The increased interest on these high performance polymers suggests their application in foams that benefit from their excellent properties. The aerospace industry has taken special notice of polyimide foams and makes use of them in very demanding applications such as thermal and acoustic insulation for various aircrafts [1,2]. Several synthetic methods for polyimide foams have been developed. Of special interest is the method developed by Weiser et al. [2,3] where polyimide foams made from powders of solid-state polyimide precursors (i.e. poly(amic acid) (PAA)) have been obtained by using tetrahydrofuran (THF) as a blowing agent that complexes through hydrogen bonding to the poly(amic acid) structure [3]. During the foaming process solid powder particles of poly(amic acid) precursors are heated from room temperature to produce microspheres and ultimately foams [2,4]. This novel approach towards the manufacture of high performance cellular materials (referred to by the authors as solid-state powder foaming) provides the base for the development of new and interesting applications. The goal of this work is to lay the groundwork for a comprehensive phenomenological analysis of the inflation process, more precisely the diffusion of volatiles through the polymeric particles, and how the balance between external desorption and internal supersaturation sets the conditions for potential inflation of precursor particles.

Solid poly(amic acid) precursors are generally obtained from the reaction of diacid–diesters of aromatic dianhydrides and aromatic diamines in what is referred to as the first of a two-step process for polyimide synthesis [5] (Fig. 1). The resultant polymer is a poly(amic acid) in solution with alcohol (obtained as a condensation byproduct), and THF as the main reaction solvent that

* Corresponding author. Tel.: +1 330 9725721; fax: +1 330 9722624.
E-mail address: cc20@uakron.edu (C.I. Cano).

0032-3861/$ - see front matter © 2005 Elsevier Ltd. All rights reserved.
doi:10.1016/j.polymer.2005.07.056

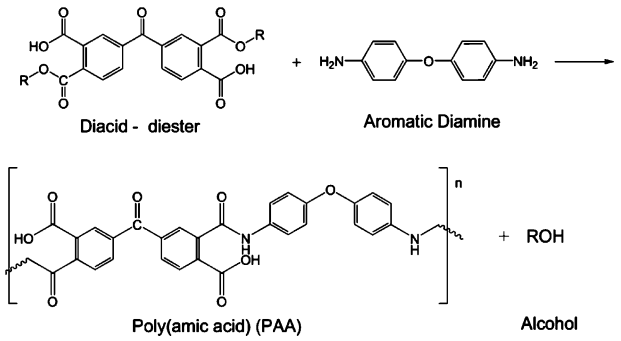

Fig. 1. Scheme of the reaction between diacid–diester compounds and aromatic diamines towards the synthesis of poly(amic acid) precursors.

subsequently acts as blowing agent. Polar solvents have been known to form strong complexes with poly(amic acid)s [6,7]. THF forms hydrogen bonds with the carboxylic and amide moieties in the PAA allowing the blowing agent to remain in situ for longer time during the subsequent foaming step. For desorption analysis, both the alcohol (i.e. methanol in the present system) and THF are regarded as the primary blowing agent due to the proximity of their boiling temperatures, and the much lower concentration of alcohol compared to THF. The polymeric solution, upon devolatilization solidifies and is comminuted to produce precursor powder fractions with particle sizes ranging from 75 to 300 μm. The devolatilization step also provides particles with interesting morphological characteristics. Comminution of brittle materials yields sharp angular particles [8]. These particles show evidence of embedded voids which become 'frozen' in the solution during the devolatilization stage as the glass transition temperature (T_g) of the system surpasses the devolatilization temperature [9]. Particles containing fragments of a different phase are referred to as 'locked' particles in the mineralogy literature [10] and this term will be utilized in this study to refer to precursor particles containing large voids. The average size of these voids ranges from the order of 0.5 to around 150 μm as evidenced by optical and electron microscopy [9].

The foaming process is carried out by heating the precursor powder containing dissolved blowing agent, above the glass transition temperature of PAA (i.e. 70–130 °C depending on the degree of plastization), and inducing inflation of the particle into a microsphere [4,9]. A subsequent temperature increase (250–300 °C) imidizes the PAA bubble into a polyimide bubble with an additional release of water as a third volatile component. Carrying out this process in a confined volume will yield neat polyimide foams as microspheres impinge and fuse to one another conforming to the shape of the mold.

The manufacture of thermoplastic foams relies heavily on the analysis and understanding of the different transport phenomena which occur together at the site of a growing bubble. Mass, heat and momentum transfer govern the rate at which bubbles grow, as well as the final dimensions they will achieve.

Bubble growth in polymeric liquids has been a fertile field of study for the past several decades [11–17]. Although the literature on bubble growth is extensive, no fundamental analysis has been developed on bubble growth during the non-isothermal transition from a solid (i.e. glassy) to a rubbery phase, while the polymeric species changes with time (i.e. transitions by curing from one polymeric species to another) and contains multi-component mixtures as the volatile species. These concurrent phenomena have not been considered in prior studies of bubble growth due to their complexity and isolated appearance in common foaming processes, and yet their interaction is the essence of the inflation phenomenon for polyimide foams produced by thermally initiated cyclation of poly(amic acid)s.

The solid state powder foaming process invokes added complexities to the inflation analysis in comparison to that of polymeric melts or solutions above T_g. During the non-isothermal process thermodynamic and kinetic transitions, as well as transport processes set the governing conditions for bubble growth and ultimately particle inflation. These conditions are of paramount importance, and constantly change when the polymeric system transforms from the glassy to the rubbery state during the actual growth of the bubble and during curing (i.e. imidization) reactions, which change the structure of the polymer. Morphological aspects of the precursor particles are also considered critical to the analysis in powder foaming given that the particles are in a comparable size scale to that of the bubbles which grow within them. This dimensional similarity of both the growing bubble and the polymer, which contains it allows a competitive phenomenon to occur where diffusion of the blowing agent is divided between diffusion into the growing bubble and diffusion towards the exterior of the particle. The extent of such competitive diffusion process determines the characteristics of the final microstructure and consequently the neat foam.

2. Experimental

Precursor particles made from poly(amic acid) of 3,3′,4,4′-benzophenonetetracarboxilic dianhydride, (BTDA) and 4,4′-oxydianiline (ODA) were manufactured and separated into different particle size fractions ranging from 75 to 300 μm (Fig. 2). The details of the manufacturing of the precursor have been discussed previously elsewhere [2,18]. Optical micrographs of the inflation process were produced in a INSTEC heating stage with an Olympus ZX-12 stereomicroscope and a Digital Instruments SPOT digital camera. Characterization of volatiles in the particles was performed based on proton nuclear magnetic resonance (^{1}H NMR) spectroscopy (Varian Mercury 300 MHz spectrometer). Thermogravimetric analysis (TGA) experiments were conducted in a Q500 TA instruments TGA with constant nitrogen flow for all experiments. Modulated

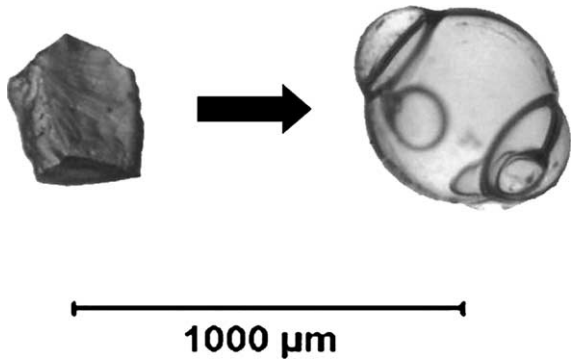

Fig. 2. Micrograph showing the morphology of a typical precursor particle and its respective mesostructure after the foaming process.

differential scanning calorimetry (MDSC) runs were conducted using a Q1000 TA instruments DSC.

2.1. Determination of global diffusion coefficients for precursor particles

Diffusivity of small molecules in polymers is affected by the inherent difficulties of transport through an entangled medium of high molecular weight species. Those difficulties are addressed in the literature by complex predictive theories that rely on many material parameters. Such material parameters are not readily available for polymer-penetrant systems with little published data such as the case of poly(amic acid) precursors and THF. Due to this, experimental determination of global diffusion coefficients has been chosen as a first approach towards the determination of diffusivities in the present system.

Experimental determination of diffusion coefficients for volatiles from polymeric systems can be performed by evaluating sorption or desorption processes. A study by Le Blevec et al. [19] uses a cell with controlled temperature and nitrogen flow to record the isothermal desorption of volatiles from polypropylene and ethylene–vinyl acetate copolymers with a gas chromatograph as the detector of the evolved species. In a similar fashion, the diffusion coefficients in the present work have been determined by thermogravimetric analysis. Assuming a spherical geometry as an approximation to the particles' average shape, the analytical solution for non-steady quiescent diffusion in a sphere may be written as [20]:

$$\frac{M_t}{M_\infty} = 1 - \frac{6}{\pi^2}\sum_{n=1}^{\infty}\frac{1}{n^2}\exp\left(\frac{-4D\pi^2 n^2}{d_p^2}t\right) \tag{1}$$

where M_t and M_∞ are the mass of diffusive substance leaving the particle at time t and the total mass of diffusive substance, respectively, while D is the diffusion coefficient and d_p is the particle size (i.e. diameter of a sphere). Rearrangement of Eq. (1) in terms of remaining weight fraction of a particle (i.e. a normalized quantity easily obtainable from TGA) yields the following expression:

$$x_{TGA} = 1 - x_i\left(1 - \frac{6}{\pi^2}\sum_{n=1}^{\infty}\frac{1}{n^2}\exp\left(\frac{-4D\pi^2 n^2}{d_p^2}t\right)\right) \tag{2}$$

where x_i is the initial mass fraction of volatiles in the sample and x_{TGA} is the remaining weight fraction at every instant t. Single particle size fractions of precursors were used in the TGA experiments allowing Eq. (2) to be solved with the assumption of a single particle size. A best fit for the diffusion coefficient may be found by minimizing the difference between the experimental data and the analytical solution. The best fit is found by minimizing an objective function S defined as [19]:

$$S = \sum_{i=1}^{z}[\ln x_{TGA-measured\ i} - \ln x_{TGA-predicted\ i}]^2 \tag{3}$$

where $x_{TGA\text{-measured}}$ is the value obtained from the TGA data at time t (corresponding to data point i), $x_{TGA\text{-predicted}}$ is the result calculated from Eq. (2) at the same time t and z is the total number of data points obtained from the TGA. Solution of Eqs. (2) and (3) was performed numerically by evaluating the series iteratively for convergence. This process was performed for different values of D until a value that minimized Eq. (3) was found.

TGA data was collected from isothermal runs at temperatures from 50 to 85 °C with sample sizes of 10–20 mg of 180 μm powder. In order to apply the analysis to the weight loss sustained only during the isothermal desorption, a weight correction was applied to account for the volatiles lost while the equipment equilibrated at the experiment's temperature. This correction consisted in using as an initial condition for the calculation the weight read by the TGA at the moment when isothermal conditions were achieved. Two main morphological assumptions are considered in the present analysis: monodispersity in the sample's particle size distribution and sphericity on the particles' shape. The former assumption is thought to be less relevant for the equation fit than the latter one, as the variation in particle size after sieving is not as wide as the variation in shape. A spherical geometry, although different in shape to the existing precursor particles, is considered a pertinent assumption that provides analytical simplicity. It is important to note that the diffusion coefficient obtained by this technique is a global coefficient and thereby represents a first-order approximation of the diffusive phenomenon in the bulk particle system.

2.2. Desorption behavior of precursor particles under non-isothermal conditions

Desorption of volatiles from the precursor particles was followed by TGA in a ramp heating procedure from room temperature to 320 °C with particles of 75, 106 and 180 μm (using samples of 10–20 mg), and heating rates of 5, 10 and 20 °C/min. Simultaneous analysis was carried out with modulated differential scanning calorimetry (MDSC) to

allow the determination of temperatures at which the evolution processes and their thermodynamic and kinetic counterparts were activated. MDSC was preferred over conventional DSC due to the overlapping of thermal phenomena such as the T_g of the PAA and volatilization of the blowing agent in the precursor system. MDSC consists of two different heating rate profiles, one linear and one oscillatory, which affects the sample differently and allow for separation of reversible and non-reversible phenomena, therefore, separating the overlapped signals. MDSC runs were performed at an underlying heating rate of 5 °C/min with amplitude of ± 0.663 °C and period of 50 s. These conditions provide an effective modulated heating profile without any cooling cycles (Fig. 3). A different set of experiments was performed on powder samples annealed previously in an oven at 70 °C for 0, 24, 36 and 72 h in order to achieve a variation in blowing agent content. TGA and MDSC analysis were performed to evaluate the dependence of the different desorption features on the blowing agent content.

3. Results and discussion

3.1. Isothermal desorption

Fig. 4 shows desorption curves for 180 μm powders at different isothermal conditions. The initial concentration of volatiles for these experiments was verified by ^{1}H NMR as 14.5% by weight. As expected, desorption rate is enhanced at higher temperatures. Global diffusion coefficients obtained from fitting Eq. (2) to the TGA data are in the order of 2×10^{-12} m^2/s for temperatures below 60 °C and increase up to $\sim 9\times10^{-12}$ m^2/s for 85 °C.

Fig. 5 shows a reasonably good agreement between the experimental data at 70 °C and the analytical solution (Eq. (2)). However, it can be seen that as the volatile concentration decreases, the solution deviates from the

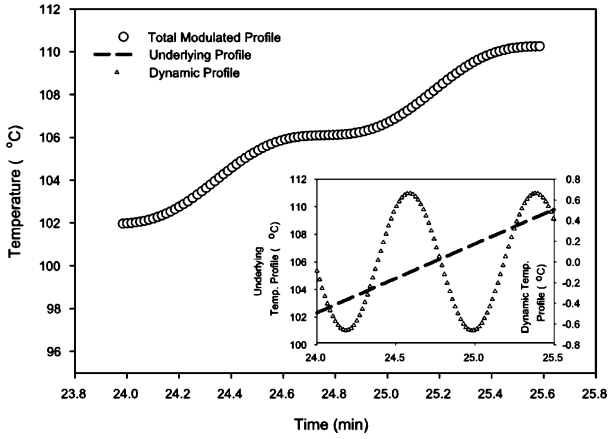

Fig. 3. Heating rate profiles used for MDSC experiments. Simultaneous heating on linear and dynamic profiles (see inset) contribute to a total modulated heating rate without any cooling stage.

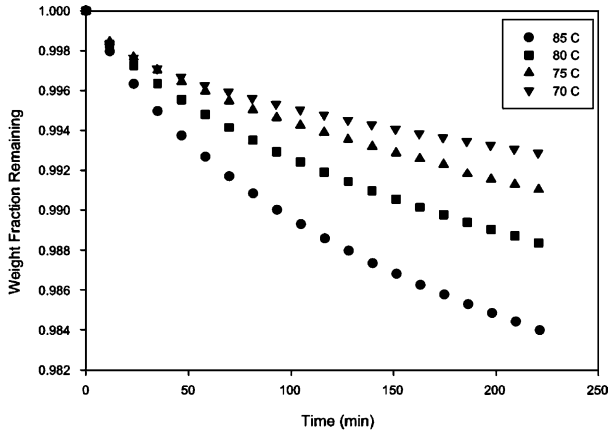

Fig. 4. Isothermal desorption curves for precursor particles obtained by TGA (D_p=180 μm).

data. Such behavior suggests a strong dependence of the diffusion coefficient on concentration, which for low penetrant concentrations should be expected. Such behavior appears to become even more critical at temperatures in the vicinity of T_g. The temperature dependence of the diffusion coefficients in polymeric systems may be expressed by:

$$D = D_0 \exp^{-(E_a/RT)} \tag{4}$$

where D_0 is a pre-exponential constant characteristic of the polymer-penetrant system, E_a is the activation energy for diffusion, R is the gas constant and T the absolute temperature. A plot of such temperature dependence for this system is presented in Fig. 6.

The expected linear behavior of Eq. (4) in a logarithmic plot is only found to exist for temperatures above 70 °C (i.e. below $1/T=2.92\times10^{-3}$ in Fig. 6), while for lower temperatures the behavior is somewhat abnormal. Instead of the increasing trend of the diffusivity versus temperature, global diffusion coefficients seem to decline with increasing temperatures below 70 °C. Such behavior is not reasonable from a phenomenological point of view as a temperature increase can only favor higher diffusivities. However, this

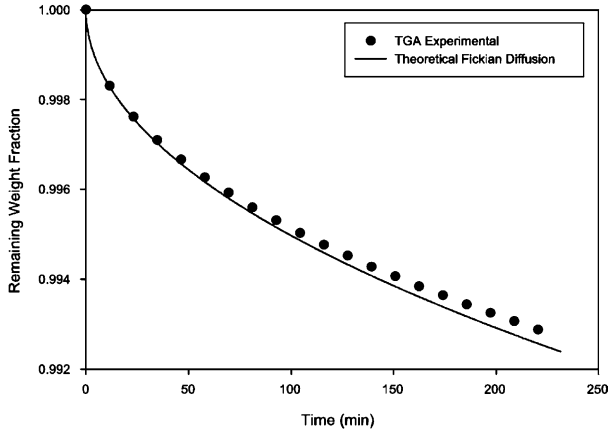

Fig. 5. Experimental and theoretical isothermal desorption of volatiles in 180 μm precursor particles at 70 °C.

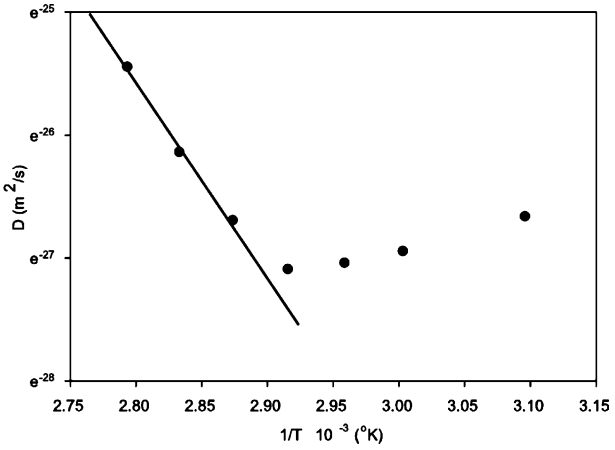

Fig. 6. Global diffusion coefficients of THF through solid precursor as a function of temperature.

observation is consistent with the fact that sorption behavior of polymer-penetrant systems below T_g is complex. Sorption theories on the glassy state such as the dual mode sorption model [21] consider that below T_g a fraction of the penetrant might be immobilized by micro-voids existing in the glassy matrix. This theory suggests that the complete concentration of volatiles determined by ^{1}H NMR and used as a base for the solution of Eq. (2) may not be available for desorption in the actual experiment at conditions below the glass transition. In addition to the possible immobilization of volatiles in the glassy polymer, complexation of THF to the poly(amic acid) also restricts mobility of the diffusant. Considering these two restrictions, the use of a previously determined initial concentration in solving Eq. (2) without considering the immobilized fractions might be responsible for the under-prediction of diffusion coefficients below T_g. The results obtained from the isothermal desorption analysis justify the validity of the proposed methodology for global diffusion coefficient measurements above T_g.

3.2. Non-isothermal desorption

Precursor particles subjected to a temperature increase will experience a buildup in temperature through its geometric profile. At the same time, Brownian motion increases as well and permits higher mobility of the chains and, therefore, enhanced diffusivity of small molecules such as the embedded blowing agent. In precursor particles the diffusion of small molecules occurs between two primary free surfaces: the external surface where the concentration of volatiles may be considered as zero, and the surface of the existing voids inside locked particles. At this inner surface the concentration of volatiles is a complex function of the solubility and partial pressure of the blowing agent in the bubble, as well as the time elapsed between the comminution of the solid-state solution and the start of the foaming process. As heating progresses, temperature and concentration profiles start to develop and the conditions for bubble growth become favorable locally in certain regions of the particle. These favorable conditions consist of a sufficiently high temperature (i.e. above the T_g of the poly(amic) acid), a decrease in viscosity and surface tension of the polymer solution and a sufficiently high concentration of volatiles to allow for partial pressure buildup inside the existing voids. Bubble growth occurs when the mechanical forces imposed by the viscosity and surface tension of the surrounding polymer, as well as the external pressure (i.e. atmospheric pressure in the present analysis) are overcome. It is important to note here that bubble nucleation has not been addressed in the present analysis due to morphological evidence that shows the presence of pre-existing nucleated bubbles inside the particles (i.e. micro and macro voids—locked particles) [9]. These bubbles may be considered in a suspended state and can be expected to resume bubble growth as soon as the appropriate conditions are reinstated.

Fig. 7 shows a typical desorption curve for ramp heating of the precursor particles at 10 °C/min. Two curves are presented: the remaining weight fraction curve and the differential thermogravimetric curve (DTG). The latter has proved of more importance in the analysis of desorption events. The first notable feature in the DTG is a small increase in the volatile evolution at low temperatures (A in Fig. 7). This first evolution peak decays and reaches a minimum at B. B is also the onset of the second evolution peak. A third desorption peak (C) is activated as the prepolymer begins the production of water during the imidization reaction when the carboxylic and amidic moieties react to form the polyimide. As mentioned before, the volatile blowing agent (i.e. THF) forms hydrogen bonds with the PAA. The presence of excess THF compared with the available carboxylic and amidic groups in the prepolymer particle means that two types of blowing agent may be present: bound and free (i.e. dissolved in the polymer) THF. It is this free THF that may diffuse at lower temperatures and accounts for the first evolution peak. Once this free blowing agent is depleted, desorption rate

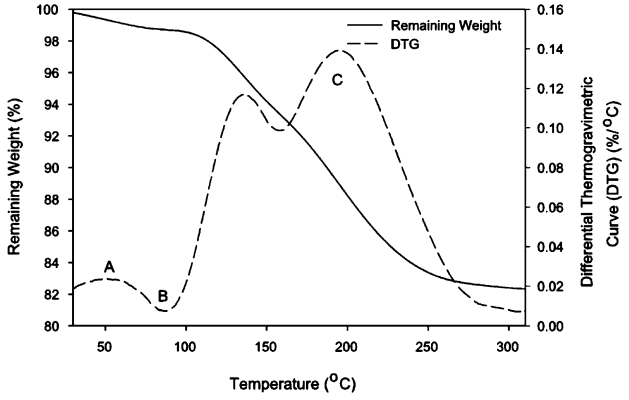

Fig. 7. Non-isothermal desorption curve for 75 μm precursor particle at 10 °C/min.

decreases until the next thermodynamic process, which is the THF decomplexation temperature. It is believed that at this point, the bound THF molecules become free as well and diffuse outwards creating the onset of the next evolution peak (point B in Fig. 7). Any remaining monomers from the initial amidation reaction (Fig. 1) may react and contribute to the second peak with alcohol vapors (i.e. byproduct of the condensation reaction).

Changes in the features of the DTG curves have been observed in response to variations of the scanning (i.e. heating) rate. Onset of desorption processes in general shift to higher temperatures as heating rate increases. This is believed to be an artifact caused by a greater difference between actual sample temperature and measured temperature as scanning rate increases. However, increases in the values of the DTG curves for desorption peaks have also been observed. These desorption increases cannot be considered artifacts but rather respond to non-isothermal kinetic phenomena such as reaction rates which depend strongly on heating rate. In order to isolate this rate-dependant behavior from the analysis of interest, care had to be taken to perform each analysis only with data from experiments performed at the same scanning rate.

Fig. 8 shows an overlay of TGA and MDSC data for a 75 μm precursor particle with reversible and non-reversible heat flows indicated. Region A in Fig. 8 corresponds to the endothermic volatilization of the blowing agent. Region B corresponds to the amidation of remaining diacid–diester groups and region C to the imidization endotherm. The peak for blowing agent devolatilization occurs almost simultaneously with the T_g of the poly(amic acid), and just before the second desorption onset. These two dynamic events act together in a synergistic fashion allowing an increased blowing agent desorption by freeing the THF and augmenting its mobility through the polymeric matrix which transitions from glassy to rubbery state. The fact that a first desorption peak (region A in Fig. 7) occurs at temperatures much lower than the T_g corroborates the assumption that only free THF is able to diffuse before the onset of the blowing agent vaporization endotherm.

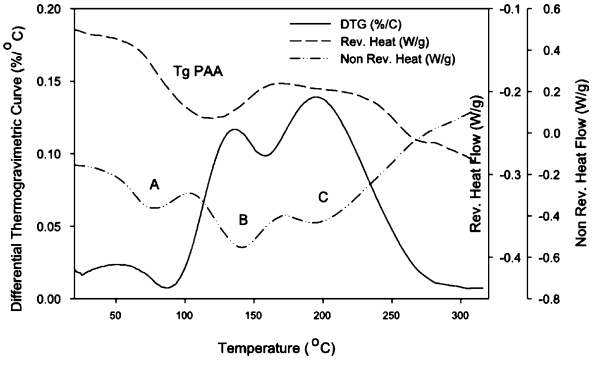

Fig. 8. TGA and MDSC overlay for 75 μm precursor particles showing reversible and non-reversible heat flows. TGA data refer to the left axis, MDSC data to the right.

The effect of particle morphology on desorption behavior may be observed from Fig. 9. Analysis by ^{1}H NMR (data not shown) presents a smaller initial blowing agent content for the smaller particles. Since all the precursor particles correspond to the same batch, this difference in concentration is attributed to ambient temperature desorption of the blowing agent during storage prior to the tests.

As described before, the volatile concentration in smaller particle sizes will change faster at a given time and temperature due to their greater specific surface. As temperature is ramped, full depletion of free blowing agent only occurs in the 75 μm particles as the other two size fractions reach the onset of volatilization and T_g before such depletion occurs. The value of the DTG at the onset of the second desorption event corresponding to the liberation of bound blowing agent is lower for 75 μm than for 106 and 180 μm. This is attributable to the significantly lower initial volatile content of the smaller fraction. However, from Fig. 9, an expected higher evolution of the volatile substance for the 180 μm particles relative to the 106 μm particles (i.e. seeing how the DTG is always higher for the 106 μm sample than the 75 μm) is not realized. This is due to the onset of bubble growth occurring in the 180 μm particles and not in the 75 or 106 μm particles.

During the bubble growth process, the competitive diffusion phenomena favors transport towards the growing bubble rather than the outer surface due to pressure and concentration differences. As the growing bubble expands and partial pressure in the bubble drops slightly, sorption equilibrium between the penetrant solubilized in the polymer and vapor in the bubble imposes a lower concentration on the bubble-polymer interface. Consequently, a higher concentration gradient (and its respective flux) develops towards the growing bubble feeding it. Growth rate in the bubble decreases eventually as less favorable mechanical conditions begin to develop

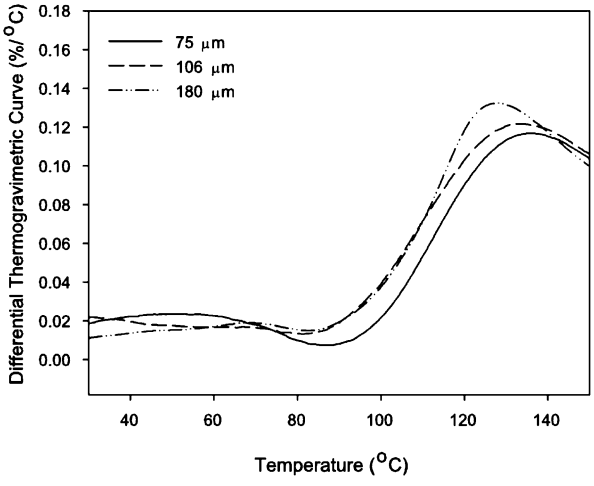

Fig. 9. Non-isothermal desorption curves for precursor particles of 75, 106 and 180 μm at 10 °C/min. Only particles of the 180 μm fraction experienced bubble growth under these conditions.

(i.e. increasing viscosity and surface tension). In the meantime, temperature (and with it internal pressure) continues increasing returning the balance of diffusion towards the outer surface once again as can be seen in Fig. 9 from the higher ultimate DTG value for the 180 μm fraction.

The effect of blowing agent content on the diffusive behavior (achieved by annealing samples at 70 °C prior to TGA and MDSC analysis) is presented on Fig. 10. As the annealing time increases (and blowing agent content decreases), desorption peaks diminish as well. The peak corresponding to free blowing agent almost disappears after the first 24 h of drying. The second desorption peak becomes lower as well indicating that decomplexation of bound THF responds to long term desorption conditions. This observation suggests again the possibility of a dual mode sorption behavior during the annealing where volatile species are not only bound to the polymer chains but also partially (instead of totally) immobilized in the micro-voids as proposed by Paul et al. [22].

4. Conclusions

Poly(amic acid) precursor particles were synthesized and separated in fractions by their particle size. Isothermal and non-isothermal desorption experiments were carried out by TGA and MDSC. Isothermal desorption experiments showed that diffusion of volatiles from the present system follows Fickian and Arrhenius-like behavior for temperatures above the corresponding glass transition temperature of the prepolymer. However, for long-term experiments, deviation from the diffusion equation occurs as depletion of volatiles proceeds suggesting a strong concentration dependence of the diffusion coefficient with concentration. Possible presence of non-Fickian diffusion in the results remains to be studied and confirmed by future work. Non-isothermal diffusive behavior is found to be more convenient for analysis by following the derivative of the weight loss (differential thermogravimetric curve) in conjunction with MDSC experiments. Activation of the desorption events has been found to correlate well with the onset of thermodynamic and kinetic transitions such as volatile vaporization, glass transition temperature of the precursor and chemical reactions of amidation and imidization. A clear difference has been found between the desorption phenomenon of free blowing agent and bound blowing agent indicating the need for a more rigorous desorption analysis that considers behavior below T_g, as well as decomplexation mechanisms.

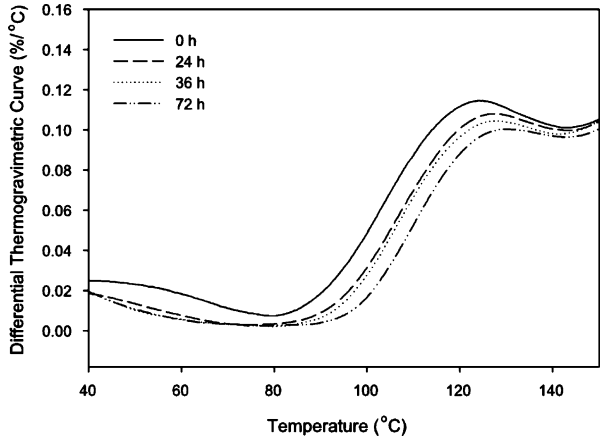

Fig. 10. Non-isothermal desorption curves for 75 μm precursor particles at 5 °C/min after different drying times at isothermal conditions prior to testing.

The presence of competitive diffusion phenomena has been corroborated through morphological dependence by favoring external desorption prior to the bubble growth and internal diffusion during the bubble growth. This occurs in clear contrast to bubble growth analysis in other processes where only diffusion into the growing bubbles was considered. The effect of particle size and shape on desorption of blowing agent, as determined by means of differential thermogravimetric plots, has been demonstrated to reveal a greater external volatile evolution prior to T_g for smaller particles. Such finding corroborates the idea of a critical particle size where external desorption prior to T_g is significant enough to hinder inflation.

The diffusive processes that govern the inflation of precursor particles by the solid-state powder foaming process are far from simple. Many concurrent phenomena add into a highly interdependent set of conditions (polymer plastization, chemical reaction, etc). The present paper attempts to give an initial approach to the dissection of all the different phenomena involved and sets the base for further individual studies.

Acknowledgements

Financial support for this work by NASA Langley Research Center (Grant No. NCC-1-02003) is gratefully acknowledged.

References

[1] McConnell VP. High Perform Compos 1997;56–8.
[2] Weiser ES, Johnson TF, Clair St TL, Echigo Y. High Perform Polym 2000;12:1–12.
[3] Weiser ES, St. Clair TL, Echigo Y, Kaneshiro H. US Patent 6′180,746 B1; 2001.
[4] Weiser ES, Grimsley BW, Pipes RB, Williams MK. Proceedings of the international SAMPE symposium. vol. 47, 2002. p. 1151–62.
[5] Sroog CE. Prog Polym Sci 1991;16:561–694.
[6] Brekner MJ, Feger C. J Polym Sci, Part A: Polym Chem 1987;25: 2005–20.
[7] Brekner MJ, Feger C. J Polym Sci, Part A: Polym Chem 1987;25: 2479–91.
[8] Meloy TP. Powder Technol 1988;55:285–91.
[9] Cano CI, Weiser ES, Pipes RB. Cell Polym 2004;23:299–309.
[10] Meloy TP, Clark NN. Part Char 1986;3:63–7.

[11] Epstein PS, Plesset MS. J Chem Phys 1950;18:1505–9.
[12] Han CD, Yoo HJ. Polym Eng Sci 1981;21:518–33.
[13] Amon M, Denson CD. Polym Eng Sci 1984;24:1026–34.
[14] Ramesh NS, Rasmussen DS, Campbell GA. Polym Eng Sci 1991;31: 1657–64.
[15] Arefmanesh A, Advani SG. Rheol Acta 1991;30:274–83.
[16] Arefmanesh A, Advani SG, Michaelides EE. Int J Heat Mass Transfer 1992;35:1711–22.
[17] Venerus DC. Polym Eng Sci 2001;41:1390–8.
[18] Cano CI, Pipes RB, Weiser ES. In: Proceedings of SPE ANTEC Technical Papers, vol. 61, 2003. p. 1835–40.
[19] Le Blevec JM, Barthel E, Briens C. Chem Eng Process 2000;39: 315–22.
[20] Crank J. The mathematics of diffusion. London: Oxford University Press; 1956 [chapter 6].
[21] Vieth WR, Sladek KJ. J Colloid Sci 1965;20:1014–33.
[22] Paul DR, Koros WJ. J Polym Sci, Part B: Polym Phys 1976;14:675.